

Extractive detoxification of hydrolysates with simultaneous formation of deep eutectic solvents

Patrycja Makoś-Chełstowska* , Edyta Słupek , Karolina Kucharska , Jacek Gębicki 

Gdansk University of Technology, Faculty of Chemistry, Department of Process Engineering and Chemical Technology, 80-233 Gdansk, Poland

*** Corresponding author:**

e-mail:

patrycja.makos@pg.edu.pl

Presented at 24th Polish Conference of Chemical and Process Engineering, 13–16 June 2023, Szczecin, Poland.

Article info:

Received: 28 April 2023

Revised: 26 June 2023

Accepted: 26 June 2023

Abstract

The hydrolysis of lignocellulosic biomass results in the production of so-called fermentation inhibitors, which reduce the efficiency of biohydrogen production. To increase the efficiency of hydrogen production, inhibitors should be removed from aqueous hydrolysate solutions before the fermentation process. This paper presents a new approach to the detoxification of hydrolysates with the simultaneous formation of *in-situ* deep eutectic solvents (DES). In the first stage of the study, inhibitors were identified in the real hydrolysate samples using high-performance liquid chromatography (HPLC). Four monoterpenes were tested for their potential to extract furfural (FF) with simultaneous DES formation. An optimization process of the most important parameters affecting the extraction process and DES formation (Thymol:FF) was conducted using the Central Composite Design (CCD) model. A temperature of 40 °C, pH of 7, $m_{\text{HBD}} : m_{\text{HYD}}$ ratio of 2:1, and time of 50 min were selected as the optimal conditions. These results indicate the high efficiency of FF removal from hydrolysates (92.1–94.6%) in a one-step process. Meanwhile, the structural properties of the formed DES measured by Fourier-transform infrared spectroscopy (FT-IR) and Nuclear magnetic resonance spectroscopy (NMR) differed only slightly from those of the DES composed of pure substances (Furfural and Thymol).

Keywords

hydrolysates, detoxification, deep eutectic solvents, furfural, fermentation

1. INTRODUCTION

Currently, biohydrogen is considered an environmentally friendly fuel with the potential to replace fossil fuels (Guo et al., 2010; Parkhey et al., 2019; Redondas et al., 2012). The two most commonly used methods for the production of hydrogen are steam-methane reforming and water electrolysis (Dash et al., 2023). However, in recent years, increasing attention has been paid to obtaining biohydrogen from waste materials using biological methods. There are environmental advantages to this solution, including the utilization of non-recyclable waste and the replacement of conventional fossil fuels with more environmentally friendly alternatives (Rathi et al., 2022). The main raw material for biohydrogen production is lignocellulosic biomass, that is, food waste, agricultural waste, or wood. The first step in the production of biohydrogen is biomass hydrolysis (Rodionova et al., 2022). During this process, lignin and hemicellulose are converted into simple fermentable sugars, including glucose, cellobiose, xylose, galactose, mannose, and arabinose. During hydrolysis, fermentation inhibitors are also generated. Phenols, polyphenols, furans, and carboxylic acids are formed, which tend to inhibit cell growth and enzymes involved in glycolysis. Consequently, fermentation inhibitors hinder biohydrogen production during fermentation. The substances occurring in high concentrations in hydrolysates that have a significant impact on reducing biohydrogen production are furans (furfural (FF)

and 5-hydroxymethylfurfural (HMF)) (Palmqvist and Hahn-Hägerdal, 2000). On the other hand, they are also valuable substances that are used in industry to produce inks, plastics, adhesives, and fertilizers, and to synthesize furfuryl alcohol, tetrahydrofuran, and levulinic acid. Therefore, the separation of furans from hydrolysates has the benefit of producing more biohydrogen, as well as obtaining valuable chemicals (Eseyin and Steele, 2015).

Currently, processes such as membrane filtration and extraction, adsorption, ion exchange, and liquid-liquid extraction (LLE) are mainly used to separate furans from aqueous solutions (Carvalho et al., 2006; Doddapaneni et al., 2018; Grzenia et al., 2012; Ludwig et al., 2013; Pan et al., 2019). Most of these processes are expensive, complicated, nonselective, and may result in sugar losses. Among the aforementioned methods, the LLE technique appears to be the most attractive because of its high selectivity and efficiency, simple recovery of FF and HMF, and low-cost procedure (Wang et al., 2021). In addition, the use of a suitable extraction solvent (non-toxic, biodegradable, low-volatility, and non-flammable) can contribute to ensuring a fully “green” process. Extraction solvents should also exhibit high affinity for furans, high hydrophobicity, and low viscosity to ensure high extraction efficiency. Conventional extraction solvents such as toluene, xylenes, ethylbenzene, isopropyl acetate, ethyl acetate, and isobutyl acetate have been studied for FF and HMF recovery



from a model or real hydrolysates. Cui et al., 2018; Dietz et al., 2019; Roque et al., 2019). However, they do not meet the standards for green chemistry and engineering. Therefore, increasing attention has been paid to the development of new alternative solvents.

Recently, compounds known as deep eutectic solvents (DES) have attracted considerable interest. DES are liquids formed by combining two or three substances, the so-called hydrogen bond donor (HBD) and hydrogen bond acceptor (HBA). Specific non-covalent interactions between HBA and HBD result in mixtures with melting points (MP) much lower than the MP of the individual components. DES have physical and chemical properties similar to those of ionic liquids (ILs); but their synthesis is much simpler and less expensive. Using substrates of natural origin renders absorbents based on DES less toxic and more biodegradable than commercial absorbents. Despite the favorable properties of DES, only a several studies on FF and HMF extraction can be found in the literature Darwish et al., 2023; Kucharska et al., 2021; Lee et al., 2019; Makoś et al., 2020; Makoś-Chełstowska et al., 2022a; McGaughy and Reza, 2020). In the mentioned papers, DES including Camphor:3,4-xyleneol (1:2), Camphor:Dodecanol (1:2), Camphor:Decanoic acid (1:2), Carvone:Menthol (1:1), Camphor:Guaiacol (1:1), Camphor:Thymol (1:1), Camphor:Octanoic acid (1:1), Choline chloride:Guaiacol (1:3) were tested. The obtained results were satisfactory, but the procedure was complex. In all studies, the procedure consisted of three steps: DES synthesis, furfural extraction, and recovery of FF and HMF from DES. The complexity of the process significantly increases the cost and execution time.

The literature data lacks studies involving simultaneous *in-situ* extraction and formation of deep eutectic solvents. The challenge of the new extraction approach is primarily the selection of an appropriate extractant that will ensure high extraction efficiency with the simultaneous formation of DES. Therefore, the paper presents research using a new approach to the extracting fermentation inhibitors by adding one substance (HBD) to an aqueous solution capable of forming hydrogen bonds with fermentation inhibitors. After combining, the substances form DES, which can be easily separated from the aqueous solution. The first stage of this study involved the identification and determination of fermentation inhibitors in various hydrolysates. Next, various substances capable of forming DES were tested under the model conditions. The substances that created the second phase after the extraction process were subjected to further analysis. An optimization procedure was performed using the Central Composite Design (CCD) model to ensure the highest extraction efficiency for fermentation inhibitors. In addition, structural studies using the FT-IR method, as well as studies of the basic physicochemical properties, including density, viscosity, and surface tension, were carried out for the formed DES. Therefore, the presented approach may be considered as a significant contribution to the field.

2. MATERIALS AND METHODS

2.1. Materials

Thymol ($\geq 98.5\%$), menthol (99.0%), eugenol (98.0%), carvone (99.0%), eucalyptol (99.0%), furfural (99.0%), 5-hydroxymethylfurfural (98.0%), 4-hydroxybenzoic acid (99.0%), vanillin (99.0%), acetonitrile ($\geq 99.9\%$), methanol ($\geq 99.9\%$), and propionic acid (99.5%) were purchased from Sigma Aldrich (St. Louis, MO, USA) and CHEMAT (Gdańsk, Poland). Sodium hydroxide (p.a) and hydrogen chloride (p.a) were purchased from Avantor Performance Materials Poland (Gliwice, Poland).

Potato pulp peelings were applied as raw materials for hydrolysis. Potato pulp contains saccharidic polymers and therefore is a nutrient medium for microorganisms (during composting) or a source of starch and lignocellulose, due to the presence of terrestrial plant parts. The handling of potato wastes is important not only because of the recovery of carbon and nitrogen sources, but also due to the environmental and water protection.

2.2. Methods

2.2.1. Hydrolysis of potato pulp peelings

Potato pulp peelings were pretreated using alkaline hydrolysis. Conditions of the process were defined in the range of three parameters, i.e. hydrolysis time 30–70 h; amount of biomass subjected to hydrolysis 1–3 g; concentration of hydrolysing agent NaOH 0.5–1.5%. For the process conditions for which the greatest changes in the polymer structure were identified, optimization of the extraction of obtained substances of secondary polysaccharide transformations was carried out (please refer to Table 1).

2.2.2. Determination and identification of fermentation inhibitors

Analysis for identification and determination of inhibitors was performed using Beckman System Gold(R) high-performance liquid chromatography (HPLC) (Beckman Coulter Inc., Fullerton, CA, USA) coupled with a single-beam system Gold 166 UV-VIS detector (Beckman Coulter Inc., Fullerton, CA, USA), a differential refractometric detector (Knauer Smartline RID 2300, Berlin, Germany), and a Kinetex 2.6 μm column, 100 \times 4.6 mm, Polar C18 100 Å (Phenomenex, Torrance, CA, USA), which was thermostated at 35 °C. The LpChrom[®] software (Lipopharm, Zblewo, Poland) was used to record and process the results.

An eluent with the composition water: methanol: acetonitrile: propionic acid (87:4:8:1 v/v) was used for HPLC analyses. Before each analysis, the model and real hydrolysate samples were filtered through a 0.45 μm hydrophilic syringe filter. The volume of the test sample was 50 μL .

2.2.3. In-situ DES preparation and extraction

Selected chemical compounds including thymol, menthol, eugenol, carvone, and eucalyptol were added to the vial with 20 mL of real or model hydrolysates. The model hydrolysate was prepared by dissolving 1 mL furfural in 200 mL water. After the addition of 20, 200, or 2000 mg of HBD to the hydrolysates, the mixture was magnetically stirred at 80 °C for 30 min.

Next, the mixture was centrifuged for 5 min at 5000 rpm. Subsequently, two phases were formed. The upper phase (DES) was transferred to a 2-mL vial and the bottom phase (hydrolysate) was filtered through a 0.45 µm syringe filter and analysed with UV-Vis detector at 284 nm. The extraction efficiency (% EE) was calculated using Equation (1).

$$EE [\%] = \frac{C_{IN} - C_{FIN}}{C_{IN}} \quad (1)$$

where: C_{IN} – initial concentration of FF in hydrolysates, g/L; C_{FIN} – concentration of FF in hydrolysates after extraction process, g/L.

2.2.4. DES characterization

Rheological and structural property tests were performed for the obtained DES in the temperature range 20–60 °C at atmospheric pressure. To study the viscosity of the DES, a viscosity meter (BROOKFIELD LVDV-II + viscometer (AMETEK Brookfield, Middleboro, MA, USA) was used. A DMA 4500 M density meter (Anton Paar, Graz, Austria) was used to determine density of DES. In addition, to determine the melting points (MP) of the new DESs, a cryostat (HUBER, Germany) was used. The DESs were cool to –30 °C and then the temperature was increased at a rate of 1 °C/min. The temperature at which a complete transition from solid to liquid was observed was considered the melting point.

The structural properties of DES were analysed using Tensor 27 FT-IR spectrometer (Bruker, Billerica, MA, USA) with an ATR adapter and OPUS software (Bruker, Billerica, MA, USA). The following FT-IR parameters were used:

spectral range, 4000–550 cm^{-1} ; resolution 4 cm^{-1} ; number of sample scans 256; number of background scans 256; slit width: 0.5 cm. The nuclear magnetic resonance spectroscopy (NMR) measurements were done at 20 °C by using Bruker Avance III HD 400 MHz (Bruker, USA). Samples for NMR analysis were prepared in 5 mm tubes by inserting 0.3 mL of DES and 0.4 mL of methanol-d1.

3. RESULTS AND DISCUSSION

3.1. Determination and identification of inhibitors fermentation

During the pretreatment of lignocellulosic biomass, a wide spectrum of additional organic compounds is created. Sugars, i.e., pentoses and hexoses undergoes secondary transformations and a group of diversified organic derivatives appears in the liquid phase. The formed organic compounds can alter the metabolic pathway of bacteria used in dark fermentation or inhibit biofuel production completely. In this study, five hydrolysates obtained after alkaline hydrolysis under various conditions were tested. Four fermentation inhibitors were identified in the samples, including FF, HMF, 4-hydroxybenzoic acid (4HBA), and vanillin (Van). FF is a dehydration product of pentoses, while HMF is formed from hexoses. The other identified fermentation inhibitors resulted from lignin decomposition.

The results are presented in Table 1. FF was present in the highest concentrations in all samples tested; therefore, FF was used for further analysis under model conditions.

3.2. In-situ DES preparation and extraction

In the first step of the study, various types of HBD were added to hydrolysate samples. The obtained results indicate that only four types of DES can be formed: Eugenol:FF, Carvone:FF, Menthol:FF, and Thymol:FF. The highest furfural extraction efficiency was obtained using thymol. Thymol has an active –OH group that can form strong hydrogen

Table 1. The content of inhibitors formed during alkaline hydrolysis.

No.	Hydrolysis time [h]	Amount of biomass [g]	Concentration of NaOH [%]	Inhibitors [mg/mL]			
				HMF	FF	4HBA	Vanillin
1	70	3	1.0	0.029	0.034	< LOD	0.004
2	70	2	1.5	0.012	0.718	0.007	< LOD
3	45	1	1.5	0.018	0.049	0.003	< LOD
4	45	3	1.5	0.041	0.098	0.004	< LOD
5	45	2	1.0	0.029	0.109	< LOD	0.003

*LOD= 0.003mg/mL (HMF); 0.002 mg/mL (FF, vanillin); 0.001 mg/mL (4HBA).

bonds with aldehyde and furan groups in the FF structure. The other HBD showed excessive water solubility and lack of affinity for FF. The addition of different amounts of FF (20 mg, 200 mg, and 2000 mg) to the model hydrolysates was tested. The results showed that as the concentration of FF increased, the extraction efficiency and formation of DES increased (Fig. 1). This was due to an increase in the number of active sites that were duplicated to form non-covalent interactions (i.e., hydrogen bonds or electrostatic interactions) with FF. Therefore, a DES consisting of 2000 mg of FF was used for further studies.

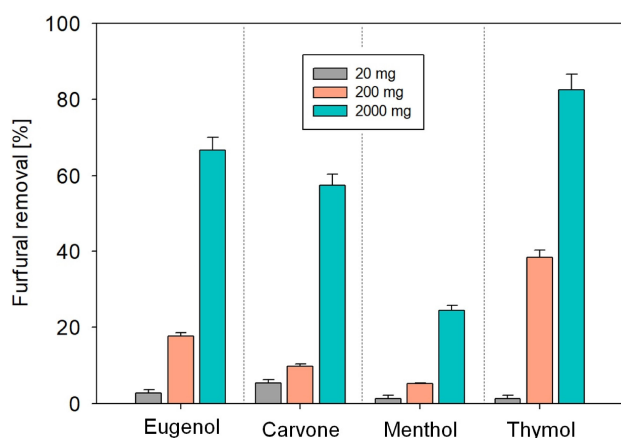


Figure 1. Extraction efficiency of furfural from model hydrolysates using various HBD.

To ensure the highest efficiency of FF removal with simultaneous DES formation, process optimization was performed using the CCD model based on previous studies (Makoś and Boczkaj, 2019; Makoś et al., 2020; Makoś-Chełstowska et al., 2022b). The experimental ranges and levels of parameters are listed in Table 2.

Table 2. Extraction efficiency of furfural from model hydrolysates using various HBD.

Variables	Coded name	Ranges and levels				
		$-\alpha$	-1	0	+1	α
Time [min]	A	10	20	30	40	50
pH [-]	B	1	4	7	10	13
Temperature [°C]	C	20	30	40	50	60
$m_{\text{HBD}} : m_{\text{HYD}}$ [-]	D	1:2	1:1	1.5:1	2:1	2.5:1

Analysis of variance (ANOVA) was performed to select the most significant parameters and their interactions affecting FF extraction. Statistical p -values and F -values were adopted as criteria at a 95% confidence level. A p -value > 0.05 was adopted as a statistically insignificant factor in the CCD model. The obtained results indicate that the prepared model was statistically significant, owing to the p -value < 0.0001 and F -value of 18.43. The p -value of the lack of error was

equal to 0.303 relative to the pure error, which means that it was statistically insignificant. The response Equation 2 obtained for the model can be expressed as follows:

$$\begin{aligned}
 Y_{FF} = & 74.66 + 0.213 \cdot A + 4.657 \cdot B - 0.073 \cdot C \\
 & + 42.24 \cdot D + 0.00387 \cdot A^2 - 0.2356 \cdot B^2 \\
 & + 0.00460 \cdot C^2 + 6.11 \cdot D^2 - 0.0371 \cdot A \cdot B \\
 & - 0.00661 \cdot A \cdot C - 0.3207 \cdot A \cdot D \\
 & - 0.0073 \cdot B \cdot C - 1.039 \cdot B \cdot D
 \end{aligned} \quad (2)$$

where: Y_{FF} – the FF extraction efficiency (%); A, B, C, D – the independent variables.

The obtained model showed a high determination coefficient R^2 of 95.18%, high values of predicted determination coefficient $R^2_{(\text{pred})}$ of 62.24%, and an adjusted determination coefficient $R^2_{(\text{adj})}$ of 90.02%. The results indicated a satisfactory correlation between the experimental results, good model fit, and the ability to predict responses to new data. The following parameters and the interactive effect of parameters were found to be significant $D, B^2, D^2, A \cdot B, A \cdot D, B \cdot D,$ and $C \cdot D$, due to a p -value lower than 0.05.

The first parameter studied was extraction time. The results showed that the efficiency of FF removal from the hydrolysates increased with increasing extraction time. A longer extraction time increased the mixing time of the solution. It is probable that an extraction time that is too short contributes to insufficient mixing (Makoś and Boczkaj, 2019). Consequently, it is not possible to properly arrange the FF and thymol molecules for the active sites to form hydrogen bonds. The maximum extraction efficiency was achieved after 50 min.

Another parameter studied was the pH of the hydrolysates. The pH was tested in the range 1–13. The results showed that a neutral pH of 7 provided the highest FF extraction efficiency. The reduced efficiency of FF removal in acidic and alkaline environments results from the fact that FF oxidizes (Dickakain, 1994). Similar results were also obtained in other works (Madani-Tonekaboni et al., 2015; Makoś et al. 2018; 2020).

The effect of temperature in the range of 20–60 °C is ambiguous and has a negligible effect on FF extraction efficiency and DES formation. On the one hand, a higher temperature favours DES formation because the synthesis procedures require elevated temperatures. In contrast, in situ DES extraction and formation can occur in two stages. Presumably, in the first step, the FF active groups ($-\text{CHO}$ and $=\text{O}$) combine with the $-\text{OH}$ hydroxyl group of FF through non-covalent bonds. This was followed in the second step by a conventional extraction process driven by the solubility of the remaining FF in DES (Th:FF). In the second stage, a theoretical increase in temperature can lower the viscosity of the DES and consequently facilitate the mass transfer process. However, the extraction process is exothermic, as

described by van't Hoff's law. According to this law, heat is released during the exothermic reaction, making the net enthalpy change negative, which directly affects the value of the partition coefficient between the DES and FF (Almashjary et al., 2018; Lozano and Martínez, 2006; Mokhtar et al., 2014). In addition, a detoxification temperature that is too high affects sugars in the hydrolysate. At temperatures that are too high, caramelization and subsequent pyrolysis of sugars can occur (Makoś et al., 2020). Therefore, 40 °C was found to be optimal.

The last parameter optimized was the mass ratio of thymol to hydrolysate. In the studied range, $m_{\text{HBD}} : m_{\text{HYD}}$ should

be 1:2. A smaller amount of thymol, despite the increase in the number of active –OH groups, is not favorable. Excessive HBD can cause competition between FF-H₂O and FF-Thy hydrogen bonds and consequently limit the ability to form DES.

The effect of the individual parameters on the efficiency of FF extraction with simultaneous DES formation is shown in Figure 2.

Finally, a temperature of 40 °C, pH 7, $m_{\text{HBD}} : m_{\text{HYD}} = 2 : 1$, and time of 50 min were selected as the optimal conditions.

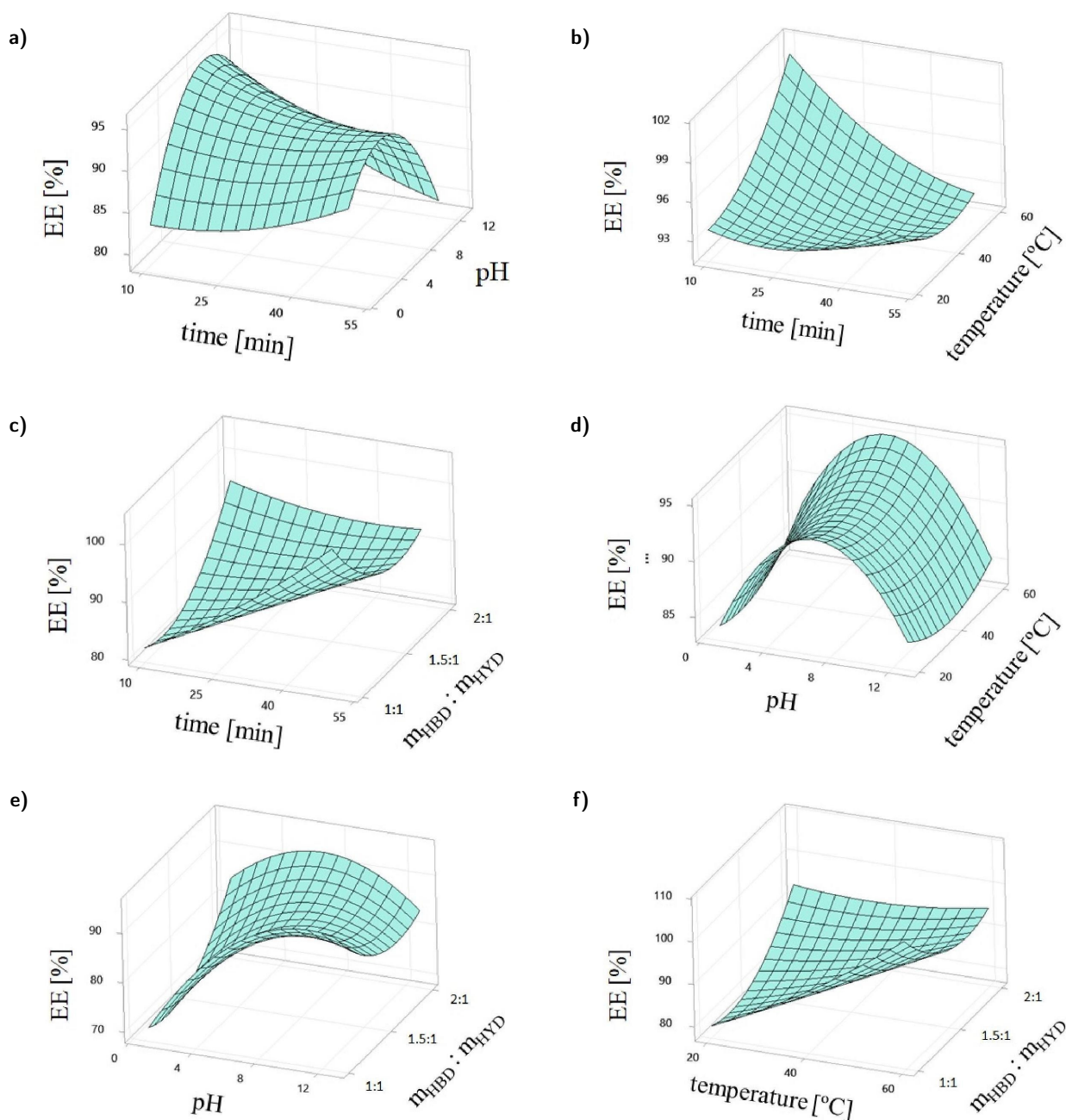


Figure 2. Response surface plots for furfural surface area dependence on a) time and pH; b) time and temperature; c) time and $m_{\text{DES}} : m_{\text{HYD}}$; d) pH and temperature; e) pH and $m_{\text{DES}} : m_{\text{HYD}}$; f) temperature and $m_{\text{DES}} : m_{\text{HYD}}$.

3.3. Application method for real samples

The optimized method was used to extract furfural and other fermentation inhibitors from the real samples. The results showed a high extraction efficiency of furfural, ranging from 92.1 to 94.6%. The slight differences are due to the presence of other inhibitors in the hydrolysates, which can block the active site of thymol ($-OH$), to which the carbonyl and aldehyde groups in the furfural structure are attached. The ex-

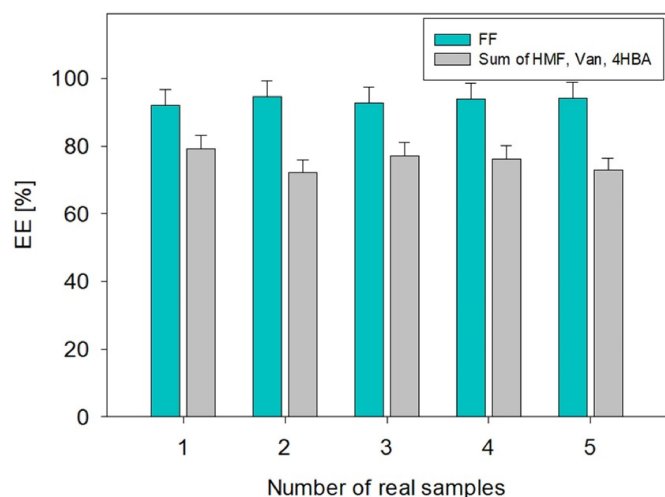


Figure 3. Extraction efficiency of FF and sum of HMF, Van, and 4HBA from real hydrolysate samples.

traction efficiencies of the other inhibitors were also high, but their concentrations were significantly lower than those of furfural. The extraction efficiency of other inhibitors decreased with increasing FF content in the hydrolysate. This indicates that DES formation is competitive with Th:FF compared to Th:Van, Th:HMF, and Th:4HBA.

3.4. DES characterization

The extraction procedure was performed under optimal conditions, and the physicochemical and structural properties of the obtained DES were characterized. All properties were determined in the temperature range of 298–328 K (Fig. 4a–4c). The analysis of physicochemical and structural properties was carried out on the DES obtained from real sample No. 2 because it had the highest furfural content and the possibility of obtaining the largest amount of sample for further studies.

The tested FF:Th showed a relatively low viscosity (7 mPa·s at 298 K), which decreases with increasing temperature (3.51 mPa·s at 328 K). The observed trend is consistent with the Arrhenius and Vogel–Fulcher–Tammann models, which show that an increase in temperature causes an increase in the average molecular velocity and a decrease in intermolecular forces in liquids, resulting in a decrease in the viscosity of the liquid (Hagbakhsh et al., 2018; Makoś-Chełstowska et al., 2021). A very similar dependence was noticeable for the

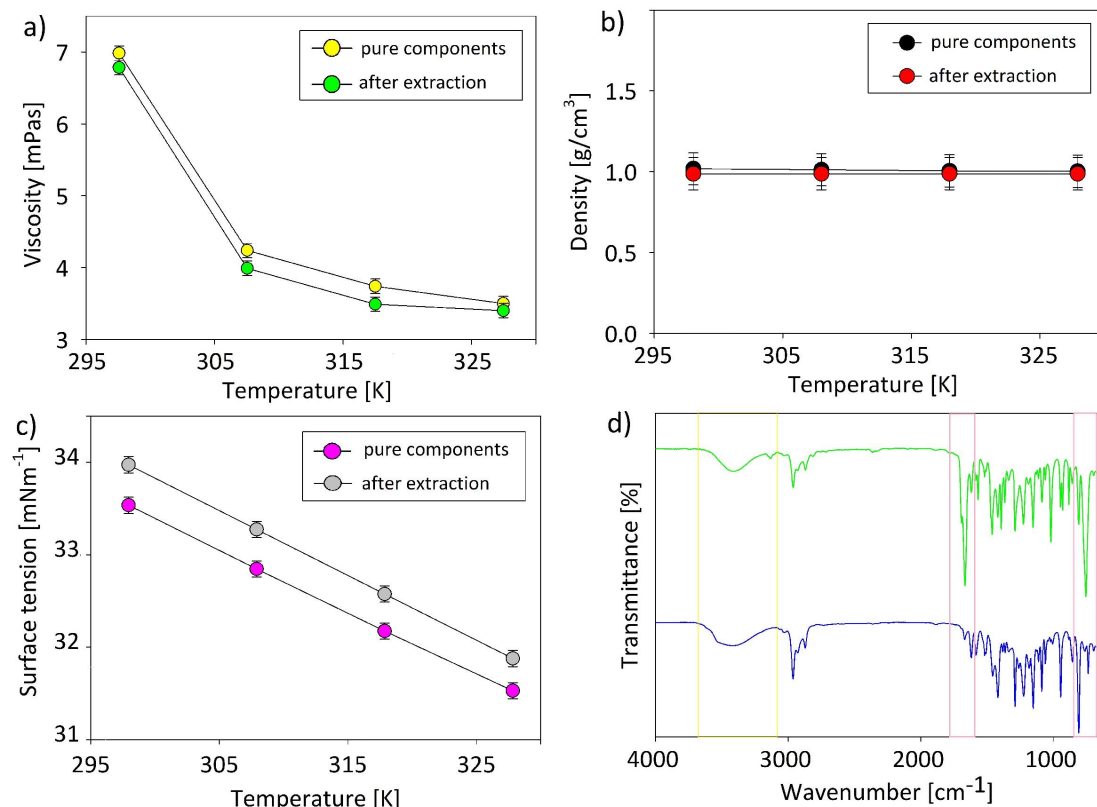


Figure 4. Physicochemical a) viscosity, b) density, c) surface tension and structural, d) FT-IR properties of the obtained DES based on FF:Th.

surface tension, which values decrease linearly with increasing temperature, from 34.00 to 31.6 mNm⁻¹ at 298 and 328 K, respectively. This phenomenon is also due to an increase in the movement of the molecules. The increased movement of the molecules causes an increase in the average kinetic energy and reduces cohesive forces. Consequently, the surface tension decreases (Abbott et al., 2006; Mjalli et al., 2014). The density values for FF:Th were practically unchanged when the temperature was increased. They were in the range of 1.03–1.01 g/cm³. The density values were close to those of water. This is of little advantage for the subsequent use of FF:Th in the extraction of other inhibitors from aqueous solutions. However, the low and constant value of the density is advantageous in terms of the use of FF:Th for other separation processes, such as absorption processes for upgrading biofuels that can be obtained with further biomass processing (Rajivgandhi and Singaravelu, 2014). The physicochemical properties of the DES were compared with those of DES obtained from pure substances. Only a slight decrease in viscosity and density and an increase in surface tension were observed. This is due to the partial solubility of water and other fermentation inhibitors in the DES.

The formation of hydrogen bonds between HBA and HBD decreases the melting point of the DES compared to the pure components. The studies showed that the newly formed DES based on FF:Th has a melting point below –30 °C, a temperature similar to the MP of pure FF, but much lower than that of pure Th.

To confirm the structure of DES, the FT-IR spectra of FF:Th obtained from pure components (green line) and those formed as a result of extraction (blue line) were compared (Fig. 4c). The FT-IR spectra showed only changes in the width and intensity of the bands, without identifying new bands that could indicate the additional formation of by-products. In the FTIR spectra, an increase in the width and intensity derived from the –OH group (3429 cm⁻¹) and the increased intensities at 1668 cm⁻¹ and 756 cm⁻¹ derived from are related to the C–H vibrations in and outside the ring plane in the thymol structure. The changes most likely resulted from water saturation of the structure of the obtained FF:Th (Cañada-Barcala et al., 2021). However, further research is required to confirm this assumption of DES structure saturation.

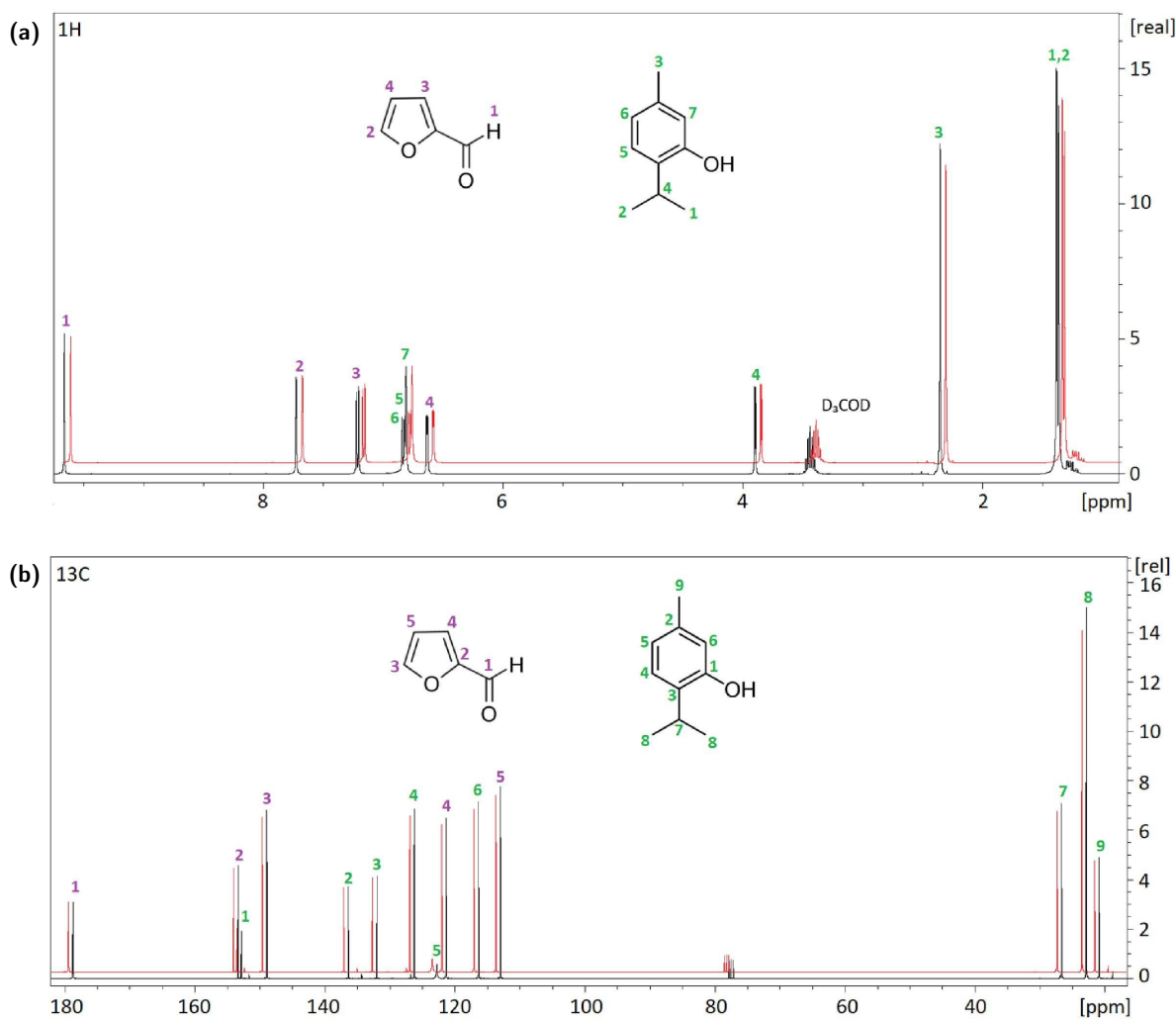


Figure 5. NMR (a) HNMR and b) CNMR) structural properties of the obtained DES based on FF:Th.

The formation of a new DES was a consequence of the formation of hydrogen bonds between HBA and HBD. NMR studies are often used to confirm the structures of new DESs. Figure 5 shows the ^1H NMR (a) and ^{13}C NMR (b) results, which show that all the identified hydrogen and carbon atoms correspond only to HBA and HBD. The absence of additional peaks confirmed that the DES was obtained without additional side reactions. In addition, Figure 5 compares the structure of the DES formed from pure components (black line) and obtained as a result of extraction (red line). No significant differences were observed between the NMR spectra.

4. CONCLUSIONS

This study presents a pioneering and innovative new approach for the detoxification of hydrolysates with the simultaneous formation of DES. In the first step, HBD was selected, which formed strong hydrogen bonds with fermentation inhibitors. Four substances from the group of monoterpenes, which are naturally derived substances with low toxicity, were tested. Based on preselection, thymol was selected because of the presence of an active $-\text{OH}$ group, which can combine with the inhibitor found at the highest concentration (FF). To increase the efficiency of hydrolysate detoxification, an optimization process was performed using the CCD model for the most relevant parameters affecting FF extraction and DES formation. A temperature of 40°C , pH of 7, $m_{\text{HBD}} : m_{\text{HYD}}$ ratio of 2:1, and time of 50 min were selected as the optimal conditions. Under such conditions, high efficiency of fermentation inhibitor removal was achieved in a one-step process. This high FF removal efficiency enabled higher biohydrogen production.

In addition, the study showed that DES obtained from samples of real hydrolysates differed only slightly from DES obtained from pure substances. Only a slight decrease in viscosity and density was observed, as well as an increase in surface tension, owing to the partial solubility of water and other inhibitors in DES. The obtained results of FF extraction confirm that the proposed new method is effective and practical, and the obtained DES can be used as extraction solvents or absorbents for other processes, such as biogas purification, which is in line with the principles of green engineering and sustainable development. On the other hand, DES, due to the presence of specific interactions between the HBD and HBA structures, can be easily separated into pure FF and thymol by reducing the temperature. This makes it possible to obtain relatively pure FF, which can be used as a raw material in the production of other chemicals or fertilizers, inks, or plastics. After separation, thymol can be recycled back into the process and reused to detoxify the hydrolysates. The presented approach should be considered as both contribution to the field and a step towards circular economy.

ACKNOWLEDGEMENTS

This research was funded by the National Science Centre, Poland within the grant project No. UMO-2021/41/B/ST8/02395.

SYMBOLS

^1H NMR	proton nuclear magnetic resonance
^{13}C NMR	carbon-13 nuclear magnetic resonance
CCD	Central Composite Design
DES	Deep Eutectic Solvents
EE	Extraction efficiency, %
FF	Furfural
FT-IR	Fourier transform infrared
HBA	Hydrogen Bond Acceptor
HBD	Hydrogen Bond Donor
HMF	5-hydroxymethylfurfural
LLE	liquid-liquid extraction
MP	melting point
Th	thymol

REFERENCES

- Abbott A.P., Capper G., Gray S., 2006. Design of improved deep eutectic solvents using hole theory. *Chem. Eur. J. of Chem. Phys.*, 7, 803–806. DOI: [10.1002/cphc.200500489](https://doi.org/10.1002/cphc.200500489).
- Almashjary K.H., Khalid M., Dharaskar S., Jagadish P., Walvekar R., Gupta T.C.S.M., 2018. Optimisation of extractive desulfurization using Choline Chloride-based deep eutectic solvents. *Fuel*, 234, 1388–1400. DOI: [10.1016/j.fuel.2018.08.005](https://doi.org/10.1016/j.fuel.2018.08.005).
- Cañada-Barcala A., Rodríguez-Llorente D., López L., Navarro P., Hernández E., Águeda V.I., Álvarez-Torrellas S., Parajó J.C., Rivas S., Larriba M., 2021. Sustainable production of furfural in biphasic reactors using terpenoids and hydrophobic eutectic solvents. *ACS Sustain. Chem. Eng.*, 9 10266–10275. DOI: [10.1021/acssuschemeng.1c02798](https://doi.org/10.1021/acssuschemeng.1c02798).
- Carvalho G.B.M., Mussatto S.I., Cândido E.J., Almeida e Silva J.B., 2006. Comparison of different procedures for the detoxification of eucalyptus hemicellulosic hydrolysate for use in fermentative processes. *J. Chem. Technol. Biotechnol.*, 81, 152–157. DOI: [10.1002/jctb.1372](https://doi.org/10.1002/jctb.1372).
- Cui P., Liu H., Xin K., Yan H., Xia Q., Huang Y., Li Q., 2018. Liquid-liquid equilibria for the ternary system of water + furfural + solvents at 303.15 and 323.15 K under atmospheric pressure. *J. Chem. Thermodyn.*, 127, 134–144. DOI: [10.1016/j.jct.2018.01.027](https://doi.org/10.1016/j.jct.2018.01.027).
- Darwish A.S., Lemaoui T., AlYammahi J., Taher H., Benguerba Y., Banat F., AlNashef I.M., 2023. Molecular insights into potential hydrophobic deep eutectic solvents for furfural extraction guided by COSMO-RS and machine learning. *J. Mol. Liq.*, 379, 121631. DOI: [10.1016/J.MOLLIQ.2023.121631](https://doi.org/10.1016/J.MOLLIQ.2023.121631).
- Dash S.K., Chakraborty S., Elangovan D., 2023. A brief review of hydrogen production methods and their challenges. *Energies*, 16, 1141. DOI: [10.3390/en16031141](https://doi.org/10.3390/en16031141).

- Dickakain G., 1994. Process for inhibiting oxidation and polymerization of furfural and its derivatives. Patent No. US5332842A.
- Dietz C.H.J.T., Gallucci F., van Sint Annaland M., Held C., Kroon M.C., 2019. 110th Anniversary: Distribution coefficients of furfural and 5-hydroxymethylfurfural in hydrophobic deep eutectic solvent + water systems: Experiments and perturbed-chain statistical associating fluid theory predictions. *Ind. Eng. Chem. Res.*, 58, 4240–4247. DOI: [10.1021/acs.iecr.8b06234](https://doi.org/10.1021/acs.iecr.8b06234).
- Doddapaneni T.R.K.C., Jain R., Praveenkumar R., Rintala J., Romar H., Konttinen J., 2018. Adsorption of furfural from torrefaction condensate using torrefied biomass. *Chem. Eng. J.*, 334, 558–568. DOI: [10.1016/j.cej.2017.10.053](https://doi.org/10.1016/j.cej.2017.10.053).
- Eseyin A.E., Steele P.H., 2015. An overview of the applications of furfural and its derivatives. *Int. J. Adv. Chem.*, 3, 42–47. DOI: [10.14419/ijac.v3i2.5048](https://doi.org/10.14419/ijac.v3i2.5048).
- Grzenia D.L., Schell D.J., Wickramasinghe S.R., 2012. Membrane extraction for detoxification of biomass hydrolysates. *Bioresour. Technol.*, 111, 248–254. DOI: [10.1016/j.biortech.2012.01.169](https://doi.org/10.1016/j.biortech.2012.01.169).
- Guo X.M., Trably E., Latrille E., Carrère H., Steyer J.-P., 2010. Hydrogen production from agricultural waste by dark fermentation: A review. *Int. J. Hydrogen Energy*, 35, 10660–10673. DOI: [10.1016/j.ijhydene.2010.03.008](https://doi.org/10.1016/j.ijhydene.2010.03.008).
- Haghighbakhsh R., Parvaneh K., Raeissi S., Shariati A., 2018. A general viscosity model for deep eutectic solvents: The free volume theory coupled with association equations of state. *Fluid Phase Equilib.*, 470, 193–202. DOI: [10.1016/j.fluid.2017.08.024](https://doi.org/10.1016/j.fluid.2017.08.024).
- Kucharska K., Makoś-Chełstowska P., Słupek E., Gębicki J., 2021. Management of dark fermentation broth via bio refining and photo fermentation. *Energies*, 14, 6268. DOI: [10.3390/en14196268](https://doi.org/10.3390/en14196268).
- Lee C.B.T.L., Wu T.Y., Ting C.H., Tan J.K., Siow L.S., Cheng C.K., Jahim J.M., Mohammad A.W., 2019. One-pot furfural production using choline chloride-dicarboxylic acid based deep eutectic solvents under mild conditions. *Bioresour. Technol.*, 278, 486–489. DOI: [10.1016/j.biortech.2018.12.034](https://doi.org/10.1016/j.biortech.2018.12.034).
- Lozano H.R., Martínez F., 2006. Thermodynamics of partitioning and solvation of ketoprofen in some organic solvent/buffer and liposome systems. *Rev. Bras. Cienc. Farm.*, 42, 601–613. DOI: [10.1590/S1516-93322006000400016](https://doi.org/10.1590/S1516-93322006000400016).
- Ludwig D., Amann M., Hirth T., Rupp S., Zibek S., 2013. Development and optimization of single and combined detoxification processes to improve the fermentability of lignocellulose hydrolysates. *Bioresour. Technol.*, 133, 455–461. DOI: [10.1016/j.biortech.2013.01.053](https://doi.org/10.1016/j.biortech.2013.01.053).
- Madani-Tonekaboni M., Kamankesh M., Mohammadi A., 2015. Determination of furfural and hydroxymethyl furfural from baby formula using dispersive liquid-liquid microextraction coupled with high performance liquid chromatography and method optimization by response surface methodology. *J. Food Compos. Anal.*, 40, 1–7. DOI: [10.1016/j.jfca.2014.12.004](https://doi.org/10.1016/j.jfca.2014.12.004).
- Makoś P., Boczkaj G., 2019. Deep eutectic solvents based highly efficient extractive desulfurization of fuels – Eco-friendly approach. *J. Mol. Liq.*, 296, 111916. DOI: [10.1016/j.molliq.2019.111916](https://doi.org/10.1016/j.molliq.2019.111916).
- Makoś P., Przyjazny A., Boczkaj G., 2018. Hydrophobic deep eutectic solvents as “green” extraction media for polycyclic aromatic hydrocarbons in aqueous samples. *J. Chromatogr. A*, 1570, 28–37. DOI: [10.1016/j.chroma.2018.07.070](https://doi.org/10.1016/j.chroma.2018.07.070).
- Makoś P., Słupek E., Gębicki J., 2020. Extractive detoxification of feedstocks for the production of biofuels using new hydrophobic deep eutectic solvents – Experimental and theoretical studies. *J. Mol. Liq.*, 308, 113101. DOI: [10.1016/j.molliq.2020.113101](https://doi.org/10.1016/j.molliq.2020.113101).
- Makoś-Chełstowska P., Słupek E., Gębicki J., 2021. Deep eutectic solvent-based green absorbents for effective volatile organochlorine compounds removal from biogas. *Green Chem.*, 23, 4814–4827. DOI: [10.1039/d1gc01735g](https://doi.org/10.1039/d1gc01735g).
- Makoś-Chełstowska P., Słupek E., Kucharska K., Kramarz A., Gębicki J., 2022a. Efficient extraction of fermentation inhibitors by means of green hydrophobic deep eutectic solvents. *Molecules*, 27, 157. DOI: [10.3390/molecules27010157](https://doi.org/10.3390/molecules27010157).
- Makoś-Chełstowska P., Słupek E., Małachowska A., 2022b. Superhydrophobic sponges based on green deep eutectic solvents for spill oil removal from water. *J. Hazard. Mater.*, 425, 127972. DOI: [10.1016/j.jhazmat.2021.127972](https://doi.org/10.1016/j.jhazmat.2021.127972).
- McCaughy K., Reza M.T., 2020. Liquid-liquid extraction of furfural from water by hydrophobic deep eutectic solvents: Improvement of density function theory modeling with experimental validations. *ACS Omega*, 5, 22305–22313. DOI: [10.1021/acsomega.0c02665](https://doi.org/10.1021/acsomega.0c02665).
- Mjalli F.S., Naser J., Jibril B., Alizadeh V., Gano Z., 2014. Tetra-butylammonium chloride based ionic liquid analogues and their physical properties. *J. Chem. Eng. Data*, 59, 2242–2251. DOI: [10.1021/je5002126](https://doi.org/10.1021/je5002126).
- Mokhtar W.N.A.W., Bakar W.A.W.A., Ali R., Kadir A.A.A., 2014. Deep desulfurization of model diesel by extraction with *N,N*-dimethylformamide: Optimization by box–Behnken design. *J. Taiwan Inst. Chem. Eng.*, 45, 1542–1548. DOI: [10.1016/J.JTICE.2014.03.017](https://doi.org/10.1016/J.JTICE.2014.03.017).
- Palmqvist E., Hahn-Hägerdal B., 2000. Fermentation of lignocellulosic hydrolysates. II: Inhibitors and mechanisms of inhibition. *Bioresour. Technol.*, 74, 25–33. DOI: [10.1016/S0960-8524\(99\)00161-3](https://doi.org/10.1016/S0960-8524(99)00161-3).
- Pan L., He M., Wu B., Wang Y., Hu G., Ma K., 2019. Simultaneous concentration and detoxification of lignocellulosic hydrolysates by novel membrane filtration system for bioethanol production. *J. Clean. Prod.*, 227, 1185–1194. DOI: [10.1016/j.jclepro.2019.04.239](https://doi.org/10.1016/j.jclepro.2019.04.239).
- Parkhey P., Mazumdar B., Mohan S.V., 2019. Chapter 15 – Exergy analysis of biomass-based hydrogen production processes, In: Pandey A., Mohan S.V., Chang J.-S., Hallenbeck P.C., Larroche C. (Eds.), *Biomass, Biofuels, Biochemicals: Biohydrogen*. Second edition. Elsevier, 383–390. DOI: [10.1016/B978-0-444-64203-5.00015-0](https://doi.org/10.1016/B978-0-444-64203-5.00015-0).
- Rajivgandhi M.M.C., Singaravelu M., 2014. Upgrading biogas to biomethane by physical absorption process. *IJAEB*, 7, 639–644. DOI: [10.5958/2230-732x.2014.01370.9](https://doi.org/10.5958/2230-732x.2014.01370.9).
- Rathi B.S., Kumar P.S., Rangasamy G., Rajendran S., 2022. A critical review on biohydrogen generation from biomass. *Int. J. Hydrogen Energy*. DOI: [10.1016/J.IJHYDENE.2022.10.182](https://doi.org/10.1016/J.IJHYDENE.2022.10.182).

Redondas V., Gómez X., García S., Pevida C., Rubiera F., Morán A., Pis J.J., 2012. Hydrogen production from food wastes and gas post-treatment by CO₂ adsorption. *Waste Manage.*, 32, 60–66. DOI: [10.1016/j.wasman.2011.09.003](https://doi.org/10.1016/j.wasman.2011.09.003).

Rodionova M.V., Bozieva A.M., Zharmukhamedov S.K., Leong Y.K., Lan J.C.-W., Veziroglu A., Veziroglu T.N., Tomo T., Chang J.-S., Allakhverdiev S.I., 2022. A comprehensive review on lignocellulosic biomass biorefinery for sustainable biofuel production. *Int. J. Hydrogen Energy*, 47, 1481–1498. DOI: [10.1016/j.ijhydene.2021.10.122](https://doi.org/10.1016/j.ijhydene.2021.10.122).

Roque L.R., Morgado G.P., Nascimento V.M., Ienczak J.L., Rabelo S.C., 2019. Liquid-liquid extraction: A promising alternative for inhibitors removing of pentoses fermentation. *Fuel*, 242, 775–787. DOI: [10.1016/j.fuel.2018.12.130](https://doi.org/10.1016/j.fuel.2018.12.130).

Wang Z., Souryadeep B., Dionisios G.V., 2021. Extraction of furfural and furfural/5-hydroxymethylfurfural from mixed lignocellulosic biomass-derived feedstocks. *ACS Sustainable Chem. Eng.*, 9, 7489–7498. DOI: [10.1021/acssuschemeng.1c00982](https://doi.org/10.1021/acssuschemeng.1c00982).